Available online at www.sciencedirect.com
ScienceDirect
Geochimica et Cosmochimica Acta 70 (2006) 4997–5012
Geochimica
www.elsevier.com/locate/gca

Rare earth element partitioning between titanite and silicate melts: Henry's law revisited

Stefan Prowatke [a,1], Stephan Klemme [b,c,*]

[a] Mineralogisches Institut, Universität Heidelberg, Im Neuenheimer Feld 236, 69120 Heidelberg, Germany
[b] Centre for Science at Extreme Conditions, University of Edinburgh, Erskine Williamson Building, Mayfield Road, Edinburgh EH9 3JZ, UK
[c] School of GeoSciences, University of Edinburgh, The Grant Institute, West Mains Rd., Edinburgh EH9 3JW, UK

Received 1 September 2005; accepted in revised form 17 July 2006

Abstract

We present detailed experimental results on the partitioning of rare earth elements (REE) between titanite and a range of different silicate melts. Our results show that Henry's law of trace element partitioning depends on bulk composition, the available partners for heterovalent substitution, crystal composition, and melt composition. We illustrate that the partition coefficients for Sm depend very strongly on the bulk concentration of Sm in the system. The substitution mechanism, by which rare earth elements are incorporated into the crystal structure, plays an important role for trace element partitioning and also for the onset of Henry's law. Our data show that there are clear differences between substitution mechanisms of major elements compared to elements which are present only as traces. Our experiments also clearly show that the onset of Henry's law depends on the concentrations of the sum of all trace elements which are incorporated into the crystal by the same substitution mechanism. For geochemical modelling of magmatic processes involving titanite, and indeed other accessory phases, it is of crucial importance to first evaluate whether the REE, and other trace elements, are present as traces or as major elements, only then appropriate D values may be chosen.

1. Introduction

Partitioning of trace elements between crystals and melts depends on melt composition (e.g., Watson, 1976; Ryerson and Hess, 1978), composition of the solid phase (e.g., Blundy and Wood, 1994) and, temperature and pressure (e.g., Adam and Green, 1994), the latter of which indirectly affects melt and crystal properties. For the interpretation of partition coefficients (D) it is also important to ascertain whether the D values obey Henry's law, and where the transition from Henry's law to non-Henry's law behaviour occurs (e.g., Mysen, 1978; Watson, 1985).

The incorporation of trace elements in a host mineral can be described thermodynamically like a solid solution. In an ideal solution, where there is no enthalpy of mixing, the activity of a component i mixing on one crystal structure site is given by Raoult's law: $a_i = X_i$, where a_i is the activity of component i and X_i is the mole fraction of i in the solid solution. If the mixing components interact with another, the activities will differ from ideal mixing. To take this into account, an activity coefficient (γ) is introduced: $a_i = \gamma_i X_i$. At high dilution, trace components become so dispersed that their presence does not affect the overall physical properties of the host mineral. The activity coefficients therefore remain constant and the activities of the trace element component are directly proportional to their concentrations. This is known as Henry's law. The simple a–X relationships in the Henry's law region, i.e. the region of high dilution, imply that an element has a partition coefficient independent of its concentration. However, increasing the trace element concentration above a critical value leads to changes of the environment of the element and causes, eventually, deviation from Henry's law. Outside Henry's law, an element will have a partition coefficient which depends on its concentration.

* Corresponding author. Fax: +44 131 6683184.
E-mail address: stephan.klemme@ed.ac.uk (S. Klemme).
[1] Present address: Swarovski, 6112 Wattens, Austria.

0016-7037/$ - see front matter © 2006 Elsevier Inc. All rights reserved.
doi:10.1016/j.gca.2006.07.016

In the late 1970s and early 1980s several studies were undertaken to study Henry's law with implications for petrogenetic modelling (Wood, 1976; Drake and Holloway, 1978; Hanson and Langmuir, 1978; Hart and Davis, 1978; Mysen, 1978; Navrotsky, 1978; Harrison and Wood, 1980; Harrison, 1981; Ray et al., 1983; Watson, 1985). Some studies report apparent non-Henry's law behaviour in compositions with very low trace element concentrations (e.g., Harrison and Wood, 1980; Urusov and Dudnikova, 1998). A study by Beattie (1993), however, showed that most of these deviations were indeed artefacts from the β-track autoradiography technique, which was used to measure the trace element concentration in the coexisting phases. Watson (1985) found no indications of non-Henry's law behaviour in the trace element signatures of natural igneous rocks. Wood (1976) suggested that the incorporation of a trace element, e.g., Sm, into a crystal structure such as garnet depends on the presence of other elements that have a similar radius and valence state and which are incorporated in the same manner like other trace element, e.g., other REE. This phenomenon was also observed by Mysen (1978), Harrison and Wood (1980) and Harrison (1981). It is interesting to note that Cr did not affect the partitioning of REE between garnet and melt, as Cr is incorporated with a different substitution mechanism (e.g., isovalent $Cr^{3+} \leftrightarrow Al^{3+}$) on another crystal site. Bindeman and Davis (2000) found no effect of doping level of REE on partitioning of Li, Rb, Sr, Ba, Ti and Zr between plagioclase and melt. However, Bindeman and Davis (2000) also show that D^{Sm} changes dramatically when the concentration of the other REE increases.

For our study we chose titanite to investigate Henry's law in more detail. Titanite ($CaTi_{1-x}Al_xSiO_4(O,OH_x,F_x)$) is an accessory phase in a wide range of igneous rocks and contains REE and HFSE from trace to major element levels. (Smith, 1970; Nakada, 1991; Paterson and Stephens, 1992; Seifert and Kramer, 2003; Vuorinen and Halenius, 2005; Seifert, 2005). To date there are no detailed studies that investigate Henry's law behaviour of trace elements in accessory phases like titanite, apatite, or rutile, although the influence of element concentration on partition coefficients is very important to consider when using partition coefficients for geochemical modelling in petrogenetic processes (e.g., Green and Pearson, 1986; Klemme et al., 2005; Prowatke and Klemme, 2006). This is especially important for accessory phases which commonly occur in rocks with very different levels of trace elements present.

Titanite, whose structure comprises chains of corner-linked titanium–oxygen octahedra, with adjacent Ti–O chains bridged by isolated silicon–oxygen tetrahedra and sevenfold coordinated calcium–oxygen polyhedra (e.g., Ribbe, 1980), has a virtually constant major element composition over a wide range of different bulk compositions (without H_2O and F in the system), temperatures and pressures (e.g., Veksler et al., 1988). This made titanite an excellent choice to study systematically the effect of melt composition on trace element composition (Prowatke and Klemme, 2005). Green and Pearson (1986) and Tiepolo et al. (2002) also studied trace element partitioning between titanite and silicate melt. Their partition coefficients are generally in good agreement with more recent results by Prowatke and Klemme (2005). However, there is some debate as to what controls partitioning. Whilst Green and Pearson (1986) and Prowatke and Klemme (2005) argued for a pronounced role of the melt composition on partition coefficients, Tiepolo et al. (2002) argued for the crystal structure and substitution mechanism as critical factors. Nevertheless, the interpretation of partition coefficients depends critically on the fact if Henry's law is followed or not.

To better constrain the limit of Henry's law, we, therefore, conducted isobaric and isothermal partitioning experiments between titanite and melt.

2. Experimental and analytical techniques

2.1. Starting materials

Three starting materials (HL22, HL24, and HL220oAl—Table 1) were chosen to investigate Henry's law behaviour. We doped the different bulk compositions with various amounts of Sm, i.e. from 20 to 80000 ppm. To study a possible influence of other trace elements on the partitioning of Sm we conducted another set of experiments, where we doped one of the starting materials (HL22) with seven different REE (La, Nd, Sm, Gd, Dy, Er and Lu). The resulting mixtures are labelled as HL22REE. The starting compositions HL22 und HL24 are similar to the compositions used by Prowatke and Klemme (2005) and differ significantly in ASI (ASI-alumina saturation index: molar ratio $Al_2O_3/(Na_2O+K_2O+CaO)$ or $Al/(Na+K+Ca/2)$), whereas the SiO_2 contents are relatively constant (Table 1). Composition HL220oAl contains no Al_2O_3, only SiO_2, Na_2O, CaO and TiO_2 (Table 1). This composition was chosen to investigate whether the absence of Al in the bulk composition has an influence on the partitioning of Sm between titanite and melt.

All three compositions were doped with different amounts of Sm ranging from 20 to about 80,000 ppm. Through very different levels doped of Sm, we set out to

Table 1
Measured major element (wt%) composition of starting materials

Sample	Series HL22	Series HL24	Series HL220oAl	Single exp. SH2Na	Single exp. SH2K
SiO_2	50.47	49.43	59.45	48.67	46.96
Al_2O_3	6.10	9.63	—	4.78	4.58
Na_2O	9.29	6.98	5.72	7.99	—
K_2O	0.79	0.77	—	—	11.89
CaO	14.50	14.10	15.11	17.02	16.32
TiO_2	18.32	18.14	18.85	20.79	19.74
Total	99.47	99.05	99.13	99.25	99.49
ASI	0.14	0.25	—	0.108	0.108

ASI: (alumina saturation index) molar ratio of $Al_2O_3/(Na_2O + K_2O + CaO)$.

investigate the substitution mechanism by which trace elements are incorporated in titanite, for instance whether there are differences between the incorporation of Sm as trace and as minor or even major element. As mentioned above, another starting material was prepared and HL22 was doped with 7 REE (La, Nd, Sm, Gd, Dy, Er and Lu) in different levels (''HL22REE-200'' contains 200 ppm of each REE, ''HL22REE-2000'' contains 2000 ppm of each REE, and ''HL22-5000REE'' 5000 ppm of each REE). With these experiments we set out to investigate a possible effect of other REE on Sm partitioning and on the onset of Henry's law.

Furthermore, we ran two additional experiments (SH2Na and SH2K) in the system SiO_2–Al_2O_3–CaO–TiO_2–Na_2O and SiO_2–Al_2O_3–CaO– TiO_2–K_2O (Table 1). These experiments were undertaken to evaluate the effect of Na as a potential substitution partner for the incorporation of REE into the titanite crystal structure. Na is expected to function as substitution partner for the incorporation of REE into the titanite structure, whereas potassium cannot enter the titanite structure. These two experiments were doped with different trace elements (LILE, REE, HFSE) to investigate possible coupling of trace elements during partitioning. Each starting composition was prepared by mixing the appropriate amounts of reagent grade oxides and carbonates ($CaCO_3$, Na_2CO_3, K_2CO_3, Al_2O_3, TiO_2 and SiO_2). Every starting composition contains a titanite component ($CaTiSiO_5$), usually 45–50 mol%. These mixtures were decarbonated at 1000 °C for 4 h, melted at 1400 °C and subsequently at 1550 °C, and then quenched to a glass. This procedure was repeated several times, with fine grinding in between. Afterwards every starting material was split into four parts, whereas three parts were doped with 80,000, 10,000 and 2000 ppm of Sm, respectively. After these procedures the three members of every series were mixed mechanically with the rest of the undoped starting material to get further diluted members. Detailed compositions of all starting materials are given in Table 1.

2.2. Experimental techniques

All high-temperature experiments were conducted at atmospheric pressure in a conventional vertical quench furnace, with a hot zone (±0.5 °C) of approximately 3 cm in length. Temperatures were measured before and after the runs with a type S (Pt–$Pt_{90}Rh_{10}$) thermocouple which was previously calibrated against the melting points of gold (1064.4 °C) and nickel (1455.0 °C) (Dinsdale, 1991). The temperature was controlled within 0.2 °C using commercially available Eurotherm controllers. Using the so-called wire-loop-technique (Corrigan and Gibb, 1979; Donaldson and Gibb, 1979) it was possible to run all samples of one series simultaneously. Experiments were conducted in a constant flow of CO_2 (ΔFMQ +5). All experiments were initially heated above their liquidus (1350–1400 °C) and subsequently cooled at constant rates of 2–3 °C per hour to 1150 °C. This particular temperature was chosen because no other phases were found to exist next to titanite in our particular bulk compositions (only the HL220oAl experiments contain some quartz crystals) and the melt fraction in the experimental run products is usually greater than 50%. Samples were held at the final run temperature for durations of up to 192 h to allow equilibration of crystalline phases and coexisting melts (see Table 2 for details). All experiments were terminated by quenching the samples into double-distilled water.

2.3. Analytical techniques

Experimental run products were mounted in epoxy and carefully polished with abrasive paper, followed by a series of water-based diamond pastes. Polished sections were carbon coated for electron microprobe analysis (EMPA) and subsequently gold coated for ion probe analysis. Glasses were analysed for major elements with a Cameca electron microprobe SX51 operated using an accelerating voltage of 15 kV and a beam current of 6 nA. To minimize alkali volatility and damage to glasses under the electron beam an area of 10 × 12 μm was scanned with a 1 μm beam. Counting times were 10 s on peak and 5 s on background for all elements, except for Sm with 40–200 s on peak and peak/2 s on background, depending on the doping level. The detection limit (3RSD of background) for Sm_2O_3 with a counting time of 200 s under these conditions is 0.17 wt%.

Major element concentrations of titanites were also determined with the electron microprobe. For mineral analyses an accelerating voltage of 15 kV, a beam current of 20 nA, and a beam with 1 μm in diameter were used. The counting times were identical, except for Al and Na with 20 s on peak and 10 s on background and Sm with 40–200 s on peak and peak/2 s on background. The detec-

Table 2
Experimental run conditions

Series	Starting temperature	Run temperature	Ramp (°C/h)	Run duration at final T (h)	Crystallization level (%)	Crystal shape	Size (μm)
HL220	1320	1150	2	192	~25	Euhedral	300 × 200
HL240	1370	1150	2	192	~30	Euhedral	150 × 100
HL220oAl	1320	1150	2	192	~25	Euhedral	40 × 40
HL22REE	1320	1150	2	192	~25	Euhedral	200 × 200
SH2K	1350	1150	2	240	~25	Euhedral	100 × 150
SH2Na	1350	1150	2	240	~25	Euhedral	200 × 200

tion limit for 200 s counting time is 0.09 wt% Sm_2O_3. The standards used were albite (Na), K-feldspar (K), corundum (Al), periclase (Mg), wollastonite (Ca, Si), rutile (Ti) and samarium-orthophosphate (Sm). The raw data were corrected with the 'PAP' software (Pouchou and Pichoir, 1984, 1985).

Trace element concentrations were determined by secondary ion mass spectrometry (SIMS) on a Cameca ims 3f ion microprobe at Heidelberg University, using a nominal 10 kV primary beam of $^{16}O^-$ ions. Positive secondary ions were accelerated to 4.5 keV. The energy window was set at 40 eV. We employed the energy filtering technique with an offset of 90 eV at a mass resolution $M/\Delta M$ (10%) of ≈400 to suppress interfering molecules and to minimise matrix effects. The primary current was 20 nA, resulting in a spatial resolution of ca. 20–25 μm diameter at the sample surface. The following masses were counted: ^{149}Sm and ratioed to measured value of ^{30}Si, as determined by EMPA. Ion yields for Sm were calibrated on synthetic glasses with dacitic compositions (DAC666 and DAC777) and on a glass with titanite composition (SPTNT1500). The Sm concentrations of these synthetic glasses were independently determined with the electron microprobe at the University of Heidelberg. These values were used to determine elemental ion yields needed for standardization during SIMS analyses (specific results will be published elsewhere). Ion yields were compared to the ion yields that were determined using the reference material NIST SRM 610 (Pearce et al., 1997). Differences were much less than 5% relative for Sm.

3. Results and discussion

3.1. Experimental results

As mentioned above, we performed three different sets of experiments to investigate the effect of bulk composition on Henry's law (HL22, HL24, HL220oAl), as well as another additional experimental series to study the effect of the presence of other REE on Henry's law (HL22REE). All experiments of series HL22, HL24, HL22REE, as well as the single experiments SH2Na and SH2K, contain only titanite coexisting with quenched melts. Only the experiments of the HL220oAl series show some 100 μm large quartz crystals as an additional phase (Fig. 1). The degree of crystallization was lower than 40% in all experiments (Table 2) and no quench crystals were present in the glass. No inclusions of rutile or Ca-perovskite were found in titanite, but small rounded inclusions of quenched melts are occasionally observed. Titanite crystal sizes range from 300 μm to about 100 μm across (Table 2).

As to the attainment of textural and chemical equilibrium in our experiments, titanite crystals are euhedral in shape and low standard deviations of major and trace element analyses of the titanites and coexisting glass (e.g., Table 11) may be taken as direct evidence for the attainment of equilibrium between crystal and melt (Fig. 1A and B).

Major element composition of the titanites and glasses are given in Tables 3–11. A significant amount of tetrahedral Ti in titanite (up to ~0.025 cations per formula unit (cpfu)) is inferred from microprobe analyses in all experiments (Veksler et al., 1988; Tiepolo et al., 2002; Prowatke and Klemme, 2005). When trace elements are present in very low concentrations (see below for a more detailed discussion), Ca, Ti, Si, Na and Al contents of the titanites does not vary significantly for one particular bulk composition (Tables 3, 5, 7, 9 and 11). Only when Sm or other REE are present in higher concentrations, i.e. as minor or major elements, the titanite major element composition changes quite drastically. In this case, the Na and Al content of the titanites increases with increasing REE content, whereas the Ca and Ti content decreases (Tables 3, 5, 7 and 9). In titanites with very high Sm content almost no fourfold coordinated Ti was found (Tables 5, 7 and 9).

Glasses are homogeneous as indicated by low standard deviations of the major element analyses (Tables 3, 6, 8, 10 and 11). During the experimental procedure we lost some Na due to its volatility at elevated temperatures. The Na-loss ranges from ~2 wt% Na_2O for series HL22 to only 1 wt% Na_2O for series HL220oAl. The Na-loss in series HL24 was only about 0.1 % (wt) Na_2O, due to a much high degree of polymerisation of the melt.

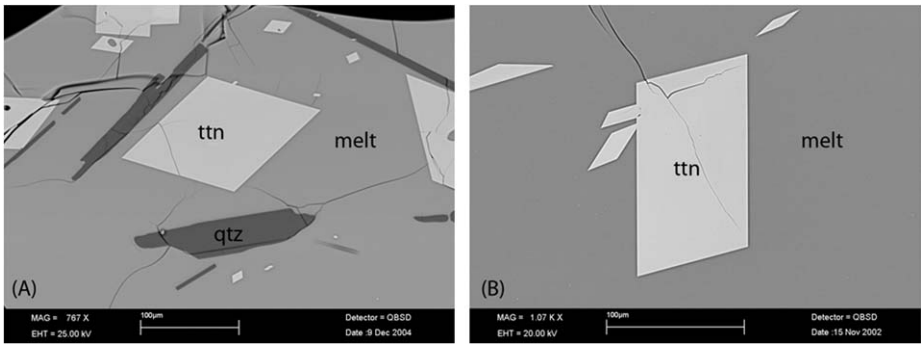

Fig. 1. Back-scattered electron images of experimental run products. (A) Run products of experiment HL220oAl. The titanite crystals are euhedral and ca. 100 μm across. Very few melt inclusions were found in these titanites. Also present are large quartz crystals. These quartz crystals contain nearly 0.4 wt% TiO_2. (B) Run products of experiment SH2K. Only titanite coexists with quenched melt. The titanites are also euhedral and contain no melt inclusions. Note that the cracks in all run products are caused by the quench procedure.

Table 3
Major and trace element content of titanites and coexisting melts of series HL22REE

Titanites	200	2000	8000	melt	200	2000	8000
Series HL22REE—EMP and SIMS analyses (wt%)— ("200, 2000 *and* 8000" *represents the doping level of each selected REE*)							
n.o.a.	(25)	(25)	(25)				
Na_2O	0.19(3)	0.25(2)	0.50(4)	Na_2O	11.84(21)	11.74(20)	11.14(18)
CaO	28.26(12)	27.47(18)	24.79(20)	CaO	8.67(17)	8.63(16)	8.59(19)
Al_2O_3	0.23(2)	0.39(2)	0.66(5)	Al_2O_3	9.28(13)	8.87(17)	8.26(14)
TiO_2	41.94(31)	41.10(25)	40.18(36)	TiO_2	8.48(17)	8.14(19)	7.50(18)
SiO_2	29.58(20)	29.23(13)	27.34(28)	SiO_2	59.88(29)	58.66(30)	54.32(25)
La_2O_3	0.014	0.16	0.49	La_2O_3	0.023	0.27	1.35
Nd_2O_3	0.028	0.30	0.92	Nd_2O_3	0.015	0.20	0.98
Sm_2O_3	0.029	0.28	0.95	Sm_2O_3	0.012	0.15	0.84
Gd_2O_3	0.028	0.25	0.92	Gd_2O_3	0.013	0.16	0.92
Dy_2O_3	0.029	0.26	0.91	Dy_2O_3	0.017	0.21	1.09
Er_2O_3	0.021	0.20	0.62	Er_2O_3	0.018	0.24	1.06
Lu_2O_3	0.013	0.12	0.36	Lu_2O_3	0.023	0.30	1.14
Total	100.37	100.01	98.65	Total	99.41	98.72	98.24
				ASI	0.254	0.245	0.235
				NBO/T	0.417	0.444	0.538
Formula (*cpfu*)				*Partition coefficients* (D^{REE}) *between ttn and melt*			
Na	0.0121	0.0160	0.0331	La	0.61(5)	0.54(2)	0.37(1)
Ca	0.9881	0.9717	0.9099	Nd	1.91(11)	1.52(5)	0.95(2)
REE	0.0018	0.0175	0.0597	Sm	2.47(17)	1.80(7)	1.12(3)
				Gd	2.16(21)	1.55(9)	1.00(4)
Total	1.0021	1.0051	1.0027	Dy	1.71(24)	1.25(9)	0.83(5)
				Er	1.14(19)	0.84(7)	0.59(4)
Ti	1.0000	1.0000	1.0000	Lu	0.55(6)	0.41(3)	0.32(1)
Total	1.0000	1.0000	1.0000				
Si	0.9651	0.9649	0.9365				
Al	0.0090	0.0151	0.0268				
Ti	0.0297	0.0208	0.0354				
Total	1.0038	1.0008	0.9987				
Total	3.0059	3.0060	3.0014				

Major elements measured with electron microprobe. REE concentrations were determined with SIMS.
n.o.a.—number of analyses (x); cpfu—cations per formula unit. All errors are 1σ, given as last significant digits in brackets (only for the major elements detecting with microprobe).

3.2. Trace element partitioning

3.2.1. Results from the starting materials HL22, HL24 and HL220oAl

Partition coefficients for the experiments of series HL22, series HL24 and HL220oAl are given in Tables 6, 8 and 10. As mentioned before, these three experimental series were performed to investigate the exact limits of Henry's law in titanite/melt partitioning experiments. Our experiments indicate that D^{Sm} in the Henry's law region depends on the bulk composition of the system. With increasing polymerisation of the melt (that is, decreasing number of non-bridging oxygen atoms per tetrahedral cation (NBO/T), or increasing alumina saturation index (ASI)) the partition coefficients increase from 0.88(3) for series HL220oAl, to 2.30(13) for series HL22, and even to 16.6(8) for series HL24 (Tables 6, 8 and 10, Fig. 2). Moreover, Fig. 2 shows that the onset of Henry's law depends on the bulk composition. In the following paragraph, we will examine the onset of Henry's law as function of bulk composition and Sm-content in titanite.

As to the bulk Sm-content, Henry's law for the HL22 experiments fails at around 5000 ppm Sm in the bulk, for the HL24 series experiments at 2000 ppm and for HL220oAl close to 2500 ppm Sm in the bulk (Fig. 2 A, B and C). The difference between HL22 and HL24 is the result of different degrees of polymerisation of the melt. However, Henry's law fails also at very low concentrations of Sm in HL220oAl series. The low Sm partition coefficients and smaller Henry's law region indicates that the presence of Al in the system affects the incorporation of REE. However, it is not entirely clear whether the presence of Al directly controls REE incorporation via Al-REE coupled substitution or whether the presence of Al only indirectly controls REE incorporation, e.g., via increasing polymerisation of the melt with increasing Al which leads to higher REE partition coefficients (Prowatke and Klemme, 2005).

Considering the onset of Henry's law as function of Sm in titanite, Henry's law fails at a Sm-content in titanite of >8000 ppm in HL22 series and HL24 series. In contrast, in the HL220oAl-series, Henry's law fails already when

Table 4
Ca-site parameters for REE^{3+} calculated with the lattice strain model (Blundy and Wood, 1994) for the series HL220REE

Series HL220REE(3+)	200	2000	8000
E^{Ca} (GPa)	539(41)	475(38)	432(58)
r_0 (Å)	1.014(1)	1.017(1)	1.016(1)
D_0	2.37(4)	1.73(3)	1.09(4)

E^{Ca}—Young's modulus; r_0 —ideal ionic radius for the given structural site; D_0—strain compensated partition coefficient.

titanite contains ~3000 ppm Sm (Fig. 2D and E). In the non-Henry's law region, however, differences between the different experimental series are small, with strongly decreasing D^{Sm} with increasing degree of polymerisation of the melt. In the HL22 series, for example, D^{Sm} decreases by a factor of ~2 from 2.30 to 0.88, whereas the partition coefficients D^{Sm} of HL24 decrease nearly by one order of magnitude from 17 to 1.7. In series HL220oAl D^{Sm} decreases by a factor of ~3 from 0.90 to 0.39.

3.2.2. Results from the starting materials HL22REE: HLREE200, HLREE2000, HLREE8000

We performed another series of experiments to investigate the effect of other trace elements on the partitioning of Sm between titanite and melt. For these experiments we chose a bulk composition identical to HL22 but added seven REE at different levels, i.e. 200 ppm, 2000 ppm, and 8000 ppm, of each REE, respectively.

Fig. 3 depicts the experimentally determined partition coefficients from these experiments. When D's are plotted versus ionic radius (Fig. 3) we find a continuous decrease of D^{REE} between titanite and melt with increasing REE content in the bulk. We have fitted the equation of the lattice strain model (Blundy and Wood, 1994; Wood and Blundy, 1997) to all experiments reported here and obtained values of D_0 (optimum partition coefficients), r_0 (optimum radius) and E (Young's modulus) for the trivalent cations which enter the Ca-position of titanite (Table 4). For a given titanite, we calculate that the Young's modulus (E) slightly decreases from 539 ± 41 to 432 ± 58 GPa with increasing REE content in titanite. The absolute values for E are consistent with results by Prowatke and Klemme (2005) and Tiepolo et al. (2002) in melts with a low degree of polymerisation. A possible explanation for the decrease of E could be the slight depolymerisation of the melt with increasing REE content (Prowatke and Klemme, 2005). The values for r_0 are constant. The D_0 values increase from 1.09 to 2.37 with decreasing REE content in the bulk.

If we plot the Sm content of titanites in the HL22REE series versus partition coefficients (Fig. 4), we observe that Henry's law fails at Sm contents in titanite less than 2500 ppm in titanite (c.f, pentagons in Fig. 4). That is con-

Table 5
Major element composition (wt%) and unit formula (apfu) of titanites of the series HL22

Series HL22 (doped Sm ppm in bulk)	Without	25	50	100	250	1500	2500	5000	15,000	40,000	60,000	75,000
n.o.a.	(30)	(30)	(30)	(30)	(30)	(30)	(30)	(30)	(30)	(30)	(30)	(30)
Na_2O	0.18(3)	0.18(3)	0.22(4)	0.19(4)	0.17(3)	0.19(3)	0.18(4)	0.25(4)	0.27(2)	0.49(3)	0.60(3)	0.66(6)
Al_2O_3	0.24(4)	0.18(3)	0.18(2)	0.19(3)	0.21(3)	0.23(3)	0.25(3)	0.35(4)	0.42(3)	0.62(4)	0.79(3)	0.99(5)
SiO_2	29.44(40)	29.32(26)	29.99(40)	29.81(30)	29.69(24)	29.60(33)	29.60(30)	29.13(33)	29.27(23)	28.88(26)	28.83(20)	28.23(26)
CaO	28.24(15)	28.64(16)	28.57(16)	28.71(17)	28.69(12)	28.57(18)	28.46(13)	28.06(13)	26.86(18)	25.41(19)	24.47(22)	23.82(26)
TiO_2	41.45(35)	41.66(30)	41.58(30)	41.77(21)	41.88(23)	41.63(34)	41.46(30)	41.53(37)	40.39(29)	39.73(31)	38.54(19)	38.56(26)
Sm_2O_3	—	—	—	—	—	0.30(7)	0.50(7)	1.08(6)	2.42(17)	4.68(19)	6.20(20)	7.49(36)
Total	99.55	99.98	100.55	100.70	100.68	100.51	100.45	100.40	99.61	99.81	99.43	99.75
Na	0.0112	0.0111	0.0137	0.0122	0.0106	0.0117	0.0117	0.0157	0.0176	0.0322	0.0396	0.0440
Ca	0.9947	1.0062	0.9961	1.0003	1.0004	0.9993	0.9970	0.9874	0.9580	0.9150	0.8915	0.8725
Sm	0.0000	0.0000	0.0000	0.0000	0.0000	0.0034	0.0056	0.0122	0.0269	0.0542	0.0726	0.0883
Total	1.0058	1.0173	1.0098	1.0126	1.0109	1.0144	1.0143	1.0153	1.0025	1.0014	1.0036	1.0048
Ti	1.0000	1.0000	1.0000	1.0000	1.0000	1.0000	1.0000	1.0000	1.0000	1.0000	0.9859	0.9918
Al	0.0000	0.0000	0.0000	0.0000	0.0000	0.0000	0.0000	0.0000	0.0000	0.0000	0.0141	0.0082
Total	1.0000	1.0000	1.0000	1.0000	1.0000	1.0000	1.0000	1.0000	1.0000	1.0000	1.0000	1.0000
Si	0.9679	0.9615	0.9757	0.9694	0.9660	0.9661	0.9676	0.9568	0.9708	0.9706	0.9802	0.9649
Al	0.0093	0.0068	0.0070	0.0073	0.0080	0.0087	0.0095	0.0136	0.0169	0.0246	0.0177	0.0316
Ti	0.0250	0.0274	0.0176	0.0219	0.0252	0.0222	0.0196	0.0262	0.0129	0.0047	0.0000	0.0000
Total	1.0022	0.9957	1.0003	0.9986	0.9992	0.9971	0.9967	0.9966	1.0006	1.0000	0.9979	0.9965
Total	3.0080	3.0133	3.0101	3.0112	3.0101	3.0115	3.0111	3.0119	3.0032	3.0014	3.0015	3.0013

The Sm_2O_3 content from experiment HL22 100–500 were below the detection limit of the microprobe. For the Sm-concentrations of these experiments see Table 6.
n.o.a.—number of analyses (x); cpfu—cations per formula unit. All errors are 1σ, given as last significant digits in brackets.

Table 6
Major element composition of titanites and melts of series HL22

Series HL22 (doped Sm ppm)	Without	25	50	100	250	1500	2500	5000	15,000	40,000	60,000	75,000
n.o.a.	(30)	(30)	(30)	(30)	(30)	(30)	(30)	(30)	(30)	(30)	(30)	(30)
Na_2O	11.98(25)	12.01(13)	12.16(17)	12.13(18)	11.99(23)	12.07(19)	11.99(17)	11.91(17)	11.45(29)	11.40(19)	10.13(21)	10.73(18)
Al_2O_3	9.41(12)	9.32(14)	9.00(11)	9.18(10)	8.86(18)	9.18(8)	9.10(14)	9.36(6)	8.77(24)	8.68(29)	7.30(15)	7.98(15)
SiO_2	59.82(36)	59.62(32)	59.31(27)	59.56(24)	59.20(28)	59.71(24)	59.78(27)	59.64(20)	58.37(39)	57.22(26)	55.51(33)	54.98(37)
K_2O	1.14(5)	1.14(4)	1.14(5)	1.15(6)	1.11(6)	1.18(6)	1.12(6)	1.11(5)	1.13(6)	1.05(4)	1.03(6)	0.98(6)
CaO	8.62(16)	8.82(14)	8.97(12)	8.90(12)	9.33(14)	8.72(11)	8.81(13)	8.59(10)	8.75(20)	8.54(12)	9.38(17)	8.94(17)
TiO_2	8.47(16)	8.64(12)	8.86(10)	8.74(14)	9.12(22)	8.59(7)	8.59(17)	8.08(10)	8.30(20)	7.64(17)	7.11(15)	7.21(15)
Sm_2O_3	—	—	—	—	—	0.14(5)	0.23(7)	0.49(9)	1.47(14)	4.63(25)	6.80(33)	8.49(29)
Total	99.45	99.55	99.45	99.66	99.62	99.58	99.61	99.18	98.23	99.15	97.27	99.32
ASI	0.257	0.252	0.240	0.245	0.234	0.248	0.246	0.257	0.244	0.245	0.210	0.228
NBO/T	0.415	0.424	0.439	0.432	0.447	0.425	0.425	0.412	0.418	0.400	0.419	0.397
Series HL22		50	100	200	500	2000	5000	10,000	22,000	45,000	65,000	80,000
Titanite		53.1(9)	111(6)	214(8)	503(19)	2490(231)	4461(321)	9440(287)				
SIMS Sm (ppm) EMS Sm_2O_3 (wt%)					0.30(7)	0.50(7)	1.08(6)	2.34(19)	4.67(25)	6.20(20)	7.49(36)	
Melt		22.0(11)	46.3(3)	87.8(18)	211(5)	1210(15)	2010(80)	4460(69)				
SIMS Sm (ppm) EMS Sm_2O_3 (wt%)					0.14(5)	0.23(7)	0.49(9)	1.55(20)	4.64(25)	6.80(37)	8.48(33)	
D^{Sm} (ttn/melt) SIMS		2.41(13)	2.40(21)	2.44(11)	2.39(21)	2.14(21)	2.22(19)	2.12(7)				
D^{Sm} (ttn/melt) EMS						2.18(94)	2.17(85)	2.20(51)	1.51(23)	1.01(6)	0.91(5)	0.88(5)

The Sm_2O_3 content from experiment SP220 100–500 were below the detection limit of the microprobe. The Sm-concentrations detecting by SIMS of these experiments are shown in the lower part of the table. Moreover the partition coefficients for Sm between titanite and melt are listed. Note that the partition coefficient of the experiments 2000–10,000 were calculated from microprobe analyses which were affected with large uncertainties. Ttn, titanite.
n.o.a.—number of analyses (x); cpfu—cations per formula unit. All errors are 1σ, given as last significant digits in brackets. 1σ uncertainty calculated by normal error propagation.

Table 7
Major element composition (wt%) and unit formula (cpfu) of titanites of the series HL24

Series HL24 (doped Sm ppm)	100	250	500	2000	5000	20,000	45,000
Na_2O	0.07(3)	0.06(1)	0.06(2)	0.07(2)	0.11(3)	0.20(4)	0.28(3)
Al_2O_3	0.30(6)	0.31(4)	0.33(4)	0.37(3)	0.51(4)	0.80(3)	1.24(7)
SiO_2	29.23(27)	29.29(14)	29.30(30)	29.34(28)	28.87(26)	28.32(37)	27.52(30)
CaO	28.56(15)	28.42(28)	28.17(22)	28.10(23)	27.42(20)	26.42(14)	24.83(21)
TiO_2	41.28(28)	41.71(31)	41.68(45)	41.24(38)	41.47(31)	39.64(48)	38.86(46)
Sm_2O_3	—	—	0.20(4)	0.56(12)	1.73(16)	3.60(19)	6.52(33)
Total	99.43	99.79	99.74	99.67	100.12	98.97	99.25
Na	0.0047	0.0040	0.0040	0.0046	0.0071	0.0131	0.0187
Ca	1.0081	0.9992	0.9914	0.9915	0.9700	0.9559	0.9114
Sm	0.0000	0.0000	0.0023	0.0064	0.0197	0.0418	0.0769
Total	1.0128	1.0032	0.9977	1.0025	0.9969	1.0108	1.0070
Ti	1.0000	1.0000	1.0000	1.0000	1.0000	1.0000	1.0000
Total	1.0000	1.0000	1.0000	1.0000	1.0000	1.0000	1.0000
Si	0.9630	0.9608	0.9623	0.9661	0.9532	0.9564	0.9429
Al	0.0116	0.0120	0.0126	0.0143	0.0200	0.0319	0.0501
Ti	0.0231	0.0296	0.0298	0.0215	0.0302	0.0071	0.0014
Total	0.9976	1.0024	1.0047	1.0019	1.0034	0.9954	0.9930
Total	3.0105	3.0056	3.0024	3.0044	3.0003	3.0062	3.0000

The Sm_2O_3 content from experiment HL24 100–500 were below the detection limit of the microprobe. For the Sm-concentrations of these experiments see Table 8.
cpfu—cations per formula unit. All errors are 1σ, given as last significant digits in brackets.

Table 8
Major element composition (wt%) of the melt of the HL24 series

	100	250	500	2000	5000	20000	45000
Series HL24 (doped Sm ppm)							
Na_2O	10.65(16)	10.55(15)	10.33(13)	10.38(16)	9.67(11)	10.75(17)	9.41(19)
Al_2O_3	15.75(20)	15.50(17)	15.83(10)	15.71(16)	15.55(21)	14.71(26)	13.26(38)
SiO_2	62.55(39)	62.70(21)	63.43(21)	63.21(37)	63.01(28)	61.57(40)	59.86(54)
K_2O	1.48(5)	1.48(4)	1.38(6)	1.38(6)	1.42(4)	1.42(6)	1.13(6)
CaO	5.69(19)	5.76(14)	5.43(9)	5.49(13)	5.95(13)	6.38(21)	7.63(36)
TiO_2	3.88(14)	3.94(23)	3.45(11)	3.55(12)	3.83(9)	3.96(13)	4.16(37)
Sm_2O_3	—	—	—	—	0.23(5)	1.10(17)	3.91(33)
Total	100.00	99.92	99.85	99.71	99.65	99.90	99.36
ASI	0.534	0.527	0.558	0.550	0.551	0.477	0.433
NBO/T	0.193	0.196	0.174	0.179	0.177	0.226	0.238
Series HL24							
Ttn							
SIMS Sm (ppm)	288(30)	692(69)	1787(167)	5133(315)	15255(1724)	33136(1462)	60747(3463)
EMP Sm_2O_3 (wt%)	—	—	0.20(4)	0.56(12)	1.73(16)	3.59(19)	6.52(33)
Melt							
SIMS Sm (ppm)	17.5(17)	42.3(34)	100(8)	322(24)	1712(103)	9387(387)	33675(492)
EMP Sm_2O_3 (wt%)	—	—	—	—	0.23(5)	1.10(17)	3.91(33)
D^{Sm} (ttn/melt)							
SIMS	16.4(23)	16.4(21)	17.8(21)	15.9(15)	8.9(11)	3.45(21)	1.80(11)
D^{Sm} (ttn/melt)							
EMP	—	—	—	—	7.5(17)	3.26(58)	1.67(16)

The Sm_2O_3 content from experiment HL24 100–2000 were below the detection limit of the microprobe (EMP). The Sm content of all experiments listed in the lower part of this table. In addition, the calculated D^{Sm} between titanite and melt are shown. Ttn, titanite.
All errors are 1σ, given as last significant digits in brackets. 1 s uncertainty calculated by normal error propagation.

Table 9
Major element composition (wt%) and unit formula (cpfu) of the synthetic titanites of the HL220oAl series

Series HL220oAl (doped Sm ppm)	100	250	500	1000	2500	5000	10,000	40,000	80,000
n.o.a.	(30)	(30)	(30)	(30)	(30)	(30)	(30)	(30)	(30)
Na_2O	0.30(5)	0.27(5)	0.31(6)	0.27(5)	0.29(4)	0.27(5)	0.37(4)	0.52(5)	0.80(2)
SiO_2	29.64(27)	29.66(27)	29.64(35)	29.59(21)	29.65(9)	29.53(27)	29.70(25)	29.20(24)	29.45(19)
K_2O	0.01(1)	0.01(1)	0.01(1)	0.01(1)	0.00(1)	0.01(1)	0.00(1)	0.01(1)	0.01(1)
CaO	27.99(21)	28.19(21)	27.99(25)	28.23(15)	27.95(4)	28.07(24)	27.08(19)	26.29(31)	25.08(15)
TiO_2	42.00(36)	42.05(36)	41.92(22)	42.05(32)	42.13(5)	41.87(38)	41.42(27)	41.03(30)	39.87(34)
Sm_2O_3	—	—	—	0.10(3)	0.33(6)	0.48(7)	1.25(16)	2.73(14)	4.70(23)
Total	99.93	100.18	99.87	100.34	100.46	100.23	99.82	99.77	99.91
Na	0.0192	0.0172	0.0195	0.0168	0.0166	0.0171	0.0235	0.0334	0.0522
Ca	0.9817	0.9869	0.9826	0.9886	0.9746	0.9851	0.9563	0.9377	0.9020
Sm	0.0000	0.0000	0.0000	0.0008	0.0045	0.0054	0.0142	0.0313	0.0544
K	0.0002	0.0002	0.0003	0.0002	0.0003	0.0003	0.0002	0.0003	0.0003
Total	1.0012	1.0045	1.0023	1.0064	0.9960	1.0079	0.9941	1.0028	1.0089
Ti	1.0000	1.0000	1.0000	1.0000	1.0000	1.0000	1.0000	1.0000	1.0000
Si	0.9704	0.9690	0.9711	0.9672	0.9783	0.9675	0.9789	0.9720	0.9885
Ti	0.0339	0.0332	0.0327	0.0334	0.0268	0.0316	0.0264	0.0272	0.0066
Total	1.0043	1.0022	1.0038	1.0006	1.0051	0.9990	1.0053	0.9992	0.9951
Total	3.0055	3.0065	3.0061	3.0074	3.0011	3.0069	2.9995	3.0020	3.0040

The Sm_2O_3 content from experiment HL220oAl 100–500 were below the detection limit of the microprobe. For the Sm-concentrations of these experiments see Table 10.
n.o.a.—number of analyses (x); cpfu—cations per formula unit. All errors are 1σ, given as last significant digits in brackets.

siderably lower when compared to our results from the HL22 series, which was doped only with Sm (c.f., circles in Fig. 4).

When we plot the entire REE content in titanite from series HL22REE versus D^{Sm} between titanite and melt we find good agreement with results from the HL22 series

Table 10
Major element composition (wt%) and "trace" element content (ppm and wt%) of titanite and melts of series HL220oAl

Series HL220oAl (doped Sm ppm)	100	250	500	1000	2500	5000	10,000	40,000	80,000
Na_2O	9.44	9.01	9.33	9.27	9.52	9.58	9.27	8.95	7.85
SiO_2	65.51	65.60	65.56	65.36	65.43	64.66	64.60	63.41	60.06
K_2O	0.44	0.79	0.56	0.77	0.47	0.34	0.36	0.42	0.38
CaO	11.47	11.45	11.38	11.37	11.27	11.66	11.06	10.81	10.28
TiO_2	11.87	11.79	11.92	12.02	11.86	11.92	11.27	10.33	8.64
Sm_2O_3	—	—	—	—	—	0.66	1.83	5.16	12.07
Total	98.73	98.63	98.76	98.80	98.54	98.82	98.39	99.07	99.29
NBO/T	0.584	0.577	0.579	0.582	0.581	0.593	0.563	0.538	0.475
Series HL220oAl	100	250	500	1000	2500	5000	10,000	25,000	50,000
Ttn									
Sm(ppm)	117(10)	249(14)	457(43)	895(54)	2689(250)	3933(175)	11329(477)	25017(1308)	
Sm_2O_3 (wt%)	—	—	—	0.10(3)	0.33(6)	0.48(7)	1.25(16)	2.73(14)	4.70(23)
Melt									
Sm(ppm)	137(7)	289(5)	500(6)	989(15)	3036(51)	5313(177)	16427(131)	45469(461)	
Sm_2O_3 (wt%)	—	—	—	—	—	0.66(7)	1.83(16)	5.16(48)	12.07(65)
D^{Sm} (ttn/melt)									
SIMS	0.85(9)	0.86(5)	0.91(9)	0.90(6)	0.89(8)	0.74(4)	0.69(3)	0.55(3)	
D^{Sm} (ttn/melt)									
EMP	—	—	—	—	—	0.74(13)	0.68(11)	0.53(5)	0.39(3)

The Sm contents of all experiments (except 50,000) were measured with SIMS. For comparison the Sm contents of the melts doped with higher Sm values were measured with electron microprobe (EMP). There is good agreement between these two analyses. The Sm-concentrations of experiment HL220oAl 100–2500 were below or near at the detection limit of the microprobe thus suffering from greater uncertainties. Furthermore, all calculated partition coefficients D^{Sm} between ttn and melt are listed. Ttn, titanite.
All errors are 1σ, given as last significant digits in brackets. 1σ uncertainty calculated by normal error propagation.

Table 11
Major and trace element composition of titanites and coexisting melt for the single experiments SH2Na and SH2K, and calculated partition coefficients (D)

Single	Titanite SH2Na	Titanite SH2K	Melt SH2Na	Melt SH2K	Doped elements	Titanite SH2Na	Melt SH2Na	Titanite SH2K	Melt SH2K	D SH2Na	D SH2K
n.o.a.	(50)	(50)	(50)	(50)		(20)	(10)	(5)	(5)		
Na_2O	0.17(3)	—	11.11(19)	0.59(4)	Rb	0.12(2)	586(3)	0.26(7)	591(3)	0.0002(1)	0.0004(1)
Al_2O_3	0.24(2)	0.27(3)	7.59(11)	7.05(13)	Sr	66(3)	155(1)	80(5)	168(2)	0.43(2)	0.48(3)
SiO_2	29.33(27)	29.71(21)	61.26(44)	58.95(36)	Y	108(6)	102(2)	76(6)	126(2)	1.06(6)	0.60(5)
K_2O	—	—	0.49(4)	14.42(19)	Zr	242(64)	158(4)	275(52)	106(3)	1.54(33)	2.58(60)
CaO	28.33(17)	28.73(19)	10.39(20)	9.93(31)	Nb	466(26)	388(19)	486(65)	485(6)	1.20(9)	1.00(13)
TiO_2	40.82(38)	40.44(34)	7.38(17)	6.60(15)	Cs	0.55(3)	292(3)	0.63(9)	213(2)	0.0018(1)	0.0029(4)
					Ba	0.95(7)	825(5)	1.32(27)	936(13)	0.0011(1)	0.0014(3)
Total	98.89	99.19	98.23	97.65	La	74(5)	151(3)	66(3)	193(2)	0.49(3)	(0.34(1)
Formula (cpfu)					Ce	81(5)	112(2)	62(3)	132(2)	0.72(5)	0.47(3)
Na	0.011	—	ASI	ASI	Pr	101(6)	90(2)	93(5)	129(2)	1.13(7)	0.72(4)
Ca	1.005	1.016	0.20	0.21	Sm	126(8)	70(2)	158(11)	152(4)	1.80(12)	1.04(8)
Total	1.016	1.016	NBO/T	NBO/T	Gd	124(8)	78(2)	76(5)	83(2)	1.60(11)	0.91(7)
			0.47	0.45	Lu	61(3)	141(2)	57(5)	222(2)	0.43(2)	0.26(2)
Ti	1.000	1.000			Hf	160(28)	73(4)	231(56)	59(3)	2.23(66)	3.92(98)
					Ta	860(50)	127(10)	691(65)	107(3)	6.78(67)	6.43(62)
Al	0.009	0.011			Pb	4.3(5)	5.0(8)	4.4(9)	5.2(7)	0.86(19)	0.88(23)
Si	0.971	0.981			Th	13.4(15)	357(3)	4.4(8)	292(3)	0.037(4)	0.015(3)
Ti	0.017	0.003			U	24.9(25)	730(3)	22.1(5)	830(10)	0.034(3)	0.027(6)
Total	0.997	0.994									

All partition coefficients between titanite and melt are listed.
n.o.a.—number of analyses (x); cpfu—cations per formula unit. All errors are 1σ, given as last significant digits in brackets. 1 s uncertainty calculated by normal error propagation.

(c.f., stars in Fig. 4). This is in good agreement with the observations by Bindeman and Davis (2000) and Wood (1976). Bindeman and Davis (2000) show that the La partition coefficient between plagioclase and silicate melt changes significantly when another REE is added to the system. They speculate that the partition coefficient of

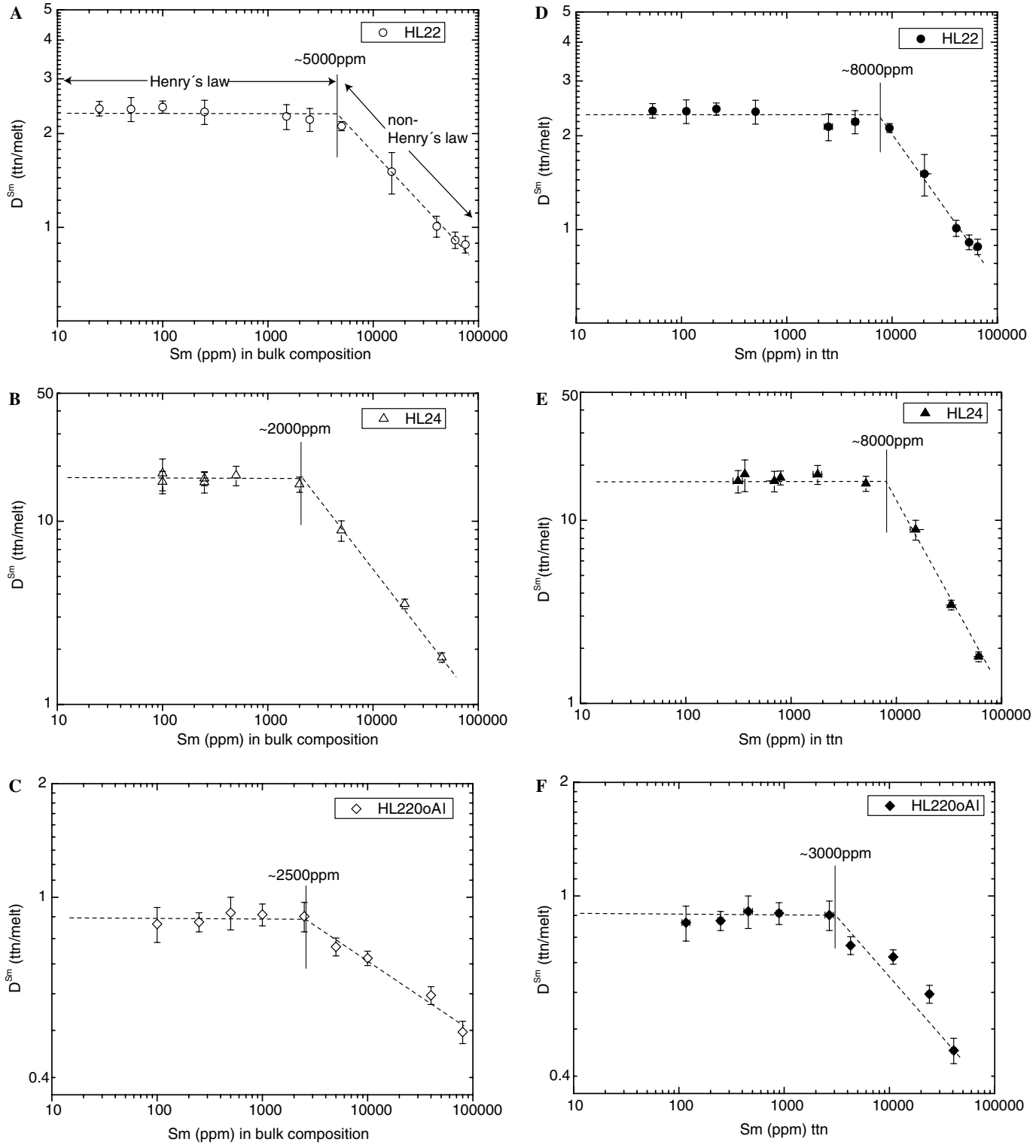

Fig. 2. (A) Sm in bulk composition plotted against D^{Sm} between titanite (ttn) and melt. The HL22 series, with a lowly polymerized melt (A), shows that Henry's law fails at a doping level of 5000 ppm in the bulk, whereas in the HL24 series, with a highly polymerized melt (B), Henry's law fails already at 2000 ppm Sm in the bulk. Moreover, we find higher D^{Sm} for the HL24 series when compared to HL22 series. This is due to different major element compositions, with higher partition coefficients in systems with melts with higher degree of polymerisation. (D and E) The Sm concentration in titanite plotted against D^{Sm} for the HL22 series and HL24 series. In both series Henry's law fails when the titanites contain about 8000 ppm Sm, which is controlled by coupled substitutions with Na and Al. See text for further discussion. In experiments without Al (with melts with low degree of polymerisation; C and F), however, Henry's law fails at much lower levels of Sm both in the bulk (C) and in titanite (F). This is due to a lack of Al in the system and, therefore, only Na (and vacancies) as potential substitution partners for Sm. See text for further discussions.

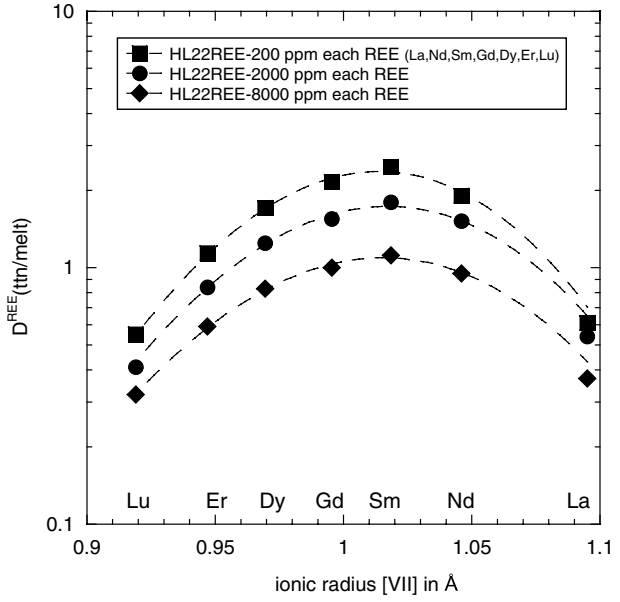

Fig. 3. Titanite/melt partition coefficients of the REE plotted against ionic radius (Shannon, 1976). We observe decreasing partition coefficients with increasing REE concentrations in the bulk. Also shown are non-linear weighted least-squares fits using the lattice strain model of Blundy and Wood (1994). Note that the parabola becomes slightly tighter with increasing REE concentration in the bulk. See Table 3 and text for further information.

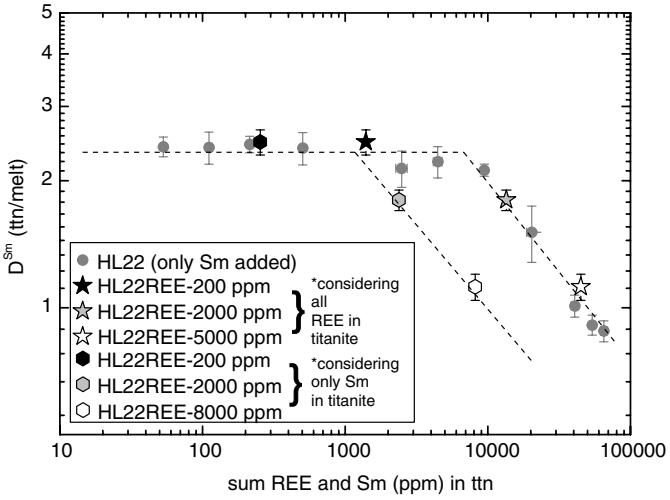

Fig. 4. D^{Sm} plotted against melt compositional parameters NBO/T (A) and ASI (B). Grey circles depict results from HL22 series, where only Sm has been added (see also Fig. 2A). Henry's law fails when titanites contain about 8000 ppm Sm. Pentagons and stars depict results from additional experiments, in the same bulk composition as HL22, but doped with seven different REE (La, Nd, Sm, Gd, Dy, Er, Lu) at strongly different levels. Considering these experiments with 7 REE added and plotting only Sm concentration in titanites (pentagons) versus D^{Sm}, we observe that Henry's law fails already at around 1000 ppm. However, when plotting the sum of all REE (stars) in titanite against D^{Sm}, we find that Henry's law holds until 8000 ppm of all REE in titanite. This indicates a very strong influence of other REE on D^{Sm}, and further substantiates the fact that the onset of Henry's law is controlled by the substitution mechanisms by which REE are incorporated into the crystal structure.

one single REE are affected by the presence of other REE due to change in the REE substitution mechanism which leads to a different activity coefficient. Fig. 4 shows that the addition of other REE also affects the onset of Henry's law. This may be explained by the fact that structural sites on which Sm is incorporated into the titanite structure are already occupied by other REE which are incorporated along the lines of the same substitution mechanism (Wood, 1976). In fact the substitution mechanism seems to be responsible for this observation (see Section 3.4 for further discussion).

3.3. The influence of melt composition on D^{Sm}

D^{Sm} from HL24 in the Henry's law region ($D^{Sm} = 16.6$) is nearly one order of magnitude larger than the D^{Sm} from HL22 ($D^{Sm} = 2.3$). The partition coefficients (D^{Sm}) of our new series agree well with the trends (see Fig. 5A and B) observed by Prowatke and Klemme (2005), but only as long as Henry's law is followed. Outside the Henry's law region D^{Sm} decreases rapidly and deviates from the observed trend (D^{Sm} vs. ASI or NBO/T) significantly (Fig. 5A and B). The rapid decrease of D^{Sm} at higher element concentrations (Fig. 5) could be explained by (1) the increasing distortion of the structure around the Ca-position in titanite, where Sm is incorporated at high levels (e.g., Tiepolo et al., 2002), (2) a change in the substitution mechanism (e.g., Beattie, 1993) (3) complexation of Sm with another major element like Al or Na in melt (e.g., Hess, 1995), or (4) the depolymerisation of the melt as Sm is known to be an network modifier (e.g., Watson, 1976). In all four scenarios, the activity coefficient of Sm (in titanite) would be affected and consequently the partition coefficient of Sm between titanite and melt would change. In this context, it should be noted that the mean value of D^{Sm} (0.88) of the HL220oAl series, a bulk composition without Al_2O_3, is slightly lower (Fig. 5) when compared to Al-bearing systems HL22 and HL24. This could be due to the absence of one potential substitution partner, in this case Al, for the heterovalent incorporation of Sm into titanite or an additional melt compositional effect.

3.4. The influence of substitution mechanism on Henry's law

In the next section, we will examine a possible role of the substitution mechanism on the onset of Henry's law. The following substitution mechanisms have been proposed for the incorporation of Sm^{3+} in titanite (Green and Pearson, 1986).

(1) Incorporation over interstitial vacancies
(2) $3Ca^{2+(VII)} \leftrightarrow \square^{(VII)} + 2Sm^{3+(VII)}$
(3) $Ca^{2+(VII)} + Ti^{4+(VI)} \leftrightarrow Sm^{3+(VII)} + Al^{3+(VI)}$
(4) $Ca^{2+(VII)} + Si^{4+(IV)} \leftrightarrow Sm^{3+(VII)} + Al^{3+(IV)}$
(5) $2Ca^{2+(VII)} \leftrightarrow Sm^{3+(VII)} + Na^{+(VII)}$

In the Henry's law region, where D^{Sm} is constant, the sum of Al+Na (cpfu), which are potential substitution partners, seems to be nearly constant over this range in all three series HL22, HL24 and HL220oAl (c.f., inlets Fig. 6A–C). In the Henry's law region the sums of Na (cpfu) and Al (cpfu) in titanite are always larger than the Sm concentration in titanite (Fig. 6). That implies that Al and Na cations in the crystal are saturated only partly through the REE, but for charge balance another substitution mechanism must apply. Alternative substitution mechanisms for Na and Al may be

$$0.5O^{2-} + (Ti^{4+}, Si^{4+}) = Al^{3+} + 0.5\square O^{2-}$$

and

$$0.5O^{2-} + Ca^{2+} = Na^{+} + 0.5\square O^{2-},$$

where the squares stand for vacancies.

However, Na seems to be absolutely independent of the Sm concentration in titanite, whereas Al may exhibit a small increase with increasing Sm concentration in titanite. We suggest that, in the Henry's law region, the Na and also the Al concentration in titanite is mainly controlled by the bulk composition, not by the substitution of elements doped at trace element level. This is consistent with the observations by Prowatke and Klemme (2005), who found virtually no dependence of the Al and Na concentration in titanite with or without the trace elements in the bulk.

In the Henry's law region, several of the aforementioned substitution mechanisms for the incorporation of Sm or REE may apply. Corgne and Wood (2005) argued that REE substitution in perovskite was controlled by the number of Ca-vacancies. A similar process could also be a viable substitution mechanism for our titanites in the Henry's law region, supported by the fact that neither Al nor Na seems to be involved for the substitution of trace elements at low concentrations. However, Al could indirectly influence the incorporation of trace elements, either by changing the melt compositions (melt compositional effect (c.f., Prowatke and Klemme, 2005)) or by stabilizing vacancies in titanite. As our experiments were conducted at relatively high temperatures, the number of intrinsic vacancies should be high which may be taken as further evidence for the presence of Ca-vacancies in titanite. Note that matters are very different in systems with much higher trace element concentrations, i.e. outside the Henry's law region (see discussion below).

3.4.1. The influence of Al on Henry's law and partition coefficients

In the next paragraph, we will examine possible reasons why D^{Sm} in Al-free systems (HL220oAl) in the Henry's law region deviate from the observed trend in Fig. 5 and why Henry's law fails at much lower Sm concentrations in titanite (Fig. 2F). To do this, we compare the experiments of series HL220oAl (in the HL-region) with experiment ASI200 by Prowatke and Klemme (2005). Melts in both experiments have identical degrees of polymerisation (i.e. NBO/T) and identical TiO_2 contents.

The only difference between these two experiments is the absence of Al in the HL220oAl series. D^{Sm} in experiment ASI200 ($D^{Sm} = 1.23$), an Al-bearing system, is nearly 40% higher than in the Henry's law region of series HL220oAl ($D^{Sm} = 0.90$). Note that the absolute concentration of Na+Al (cpfu) in the titanite in experiment ASI200 is higher than the Na content in the titanite of the HL220oAl series. It seems that more potential substitution partners are available in titanites in the Al-bearing system, which may explain higher D^{Sm}. The higher availability of

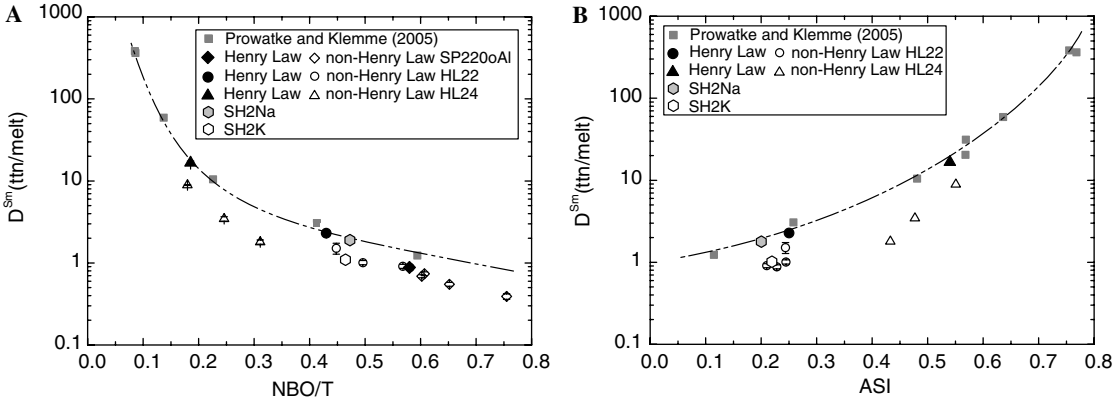

Fig. 5. Variation of D^{Sm} with (A) NBO/T and (B) aluminium saturation index (ASI = $Al_2O_3/(CaO + Na_2O + K_2O)$ molar) of melts. Grey squares were taken from Prowatke and Klemme (2005), all experiments were within Henry's law. The filled black symbols indicate averages of D^{Sm} from experiments within the Henry's law region. Two data sets (triangle-HL24, circle-HL22) plot well on the observed trend. A deviation is observed for the experiments of series HL220oAl (black diamond). The reason for that could be the absence of Al in the system. See text for further discussion. The open symbols mark experimental results outside Henry's law. These data points exhibit much lower partition coefficients. The two hexagons belong to two single experiments, SH2Na (grey) and SH2K (open). The grey hexagons plots well on the Henry's law trend. However, the open hexagons plot clearly lower, although within Henry's law. This is caused by a lack of Na in the system, and therefore limited possibility for coupled substitution. For further discussion see text.

different potential substitution partners could also explain why Henry's law fails at lower Sm concentration in the HL220oAl series (Fig. 2F). Alternatively, the presence of Al in titanite may stabilize intrinsic Ca-vacancies which control the incorporation of REE by charge-balanced substitution.

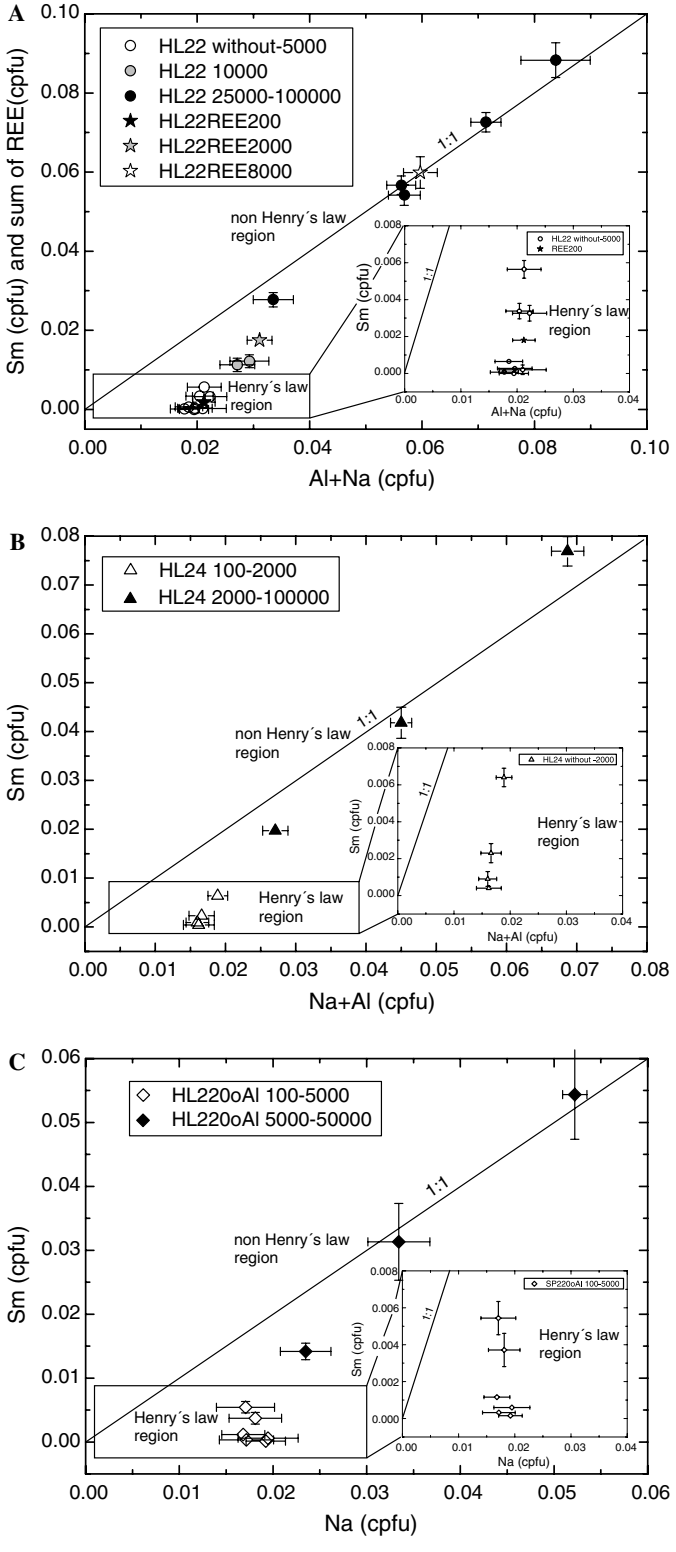

Fig. 6. Correlations between Al+Na (cpfu) and Sm (cpfu) in titanite for all three experimental series. All experiments show that the sum of Na+Al in the Henry's law region (see inlet) is always larger than the Sm content in titanite. Furthermore, Na+Al in the Henry's law region seems to be independent of the Sm concentration in titanite. Outside Henry's law there is a strong correlation between Na+Al and Sm in titanite, which indicates that the substitution mechanism controls partitioning. (A) Experiments of the HL22 series, with melts of a low degree of polymerisation. At low Sm concentrations (inlet) the partitioning follows Henry's law, at higher Sm concentrations the substitution mechanism changes and partition coefficients a driven by the coupled substitution of Na and Al with Sm. Also given here (stars) are experimental results from experiments, where seven REE were added (HL22REE200-HL22REE5000). The latter experiments plot on the same trend. (B) Experiments of the HL24 series, with melts of higher degree of polymerisation. (C) Experiments of the HL220oAl series, without Al in the bulk.

3.4.2. The influence of Na on Henry's law and partition coefficients

To investigate whether Na has an influence on Henry's law in our experiments we conducted two additional experiments (SH2K and SH2Na) in the system SiO_2–Al_2O_3–CaO–TiO_2–K_2O and SiO_2–Al_2O_3–CaO–TiO_2–Na_2O). Both experiments were doped with a range of trace elements (Table 11) to investigate if Na controls partition coefficients via a coupled substitution with REE (Fig. 7). Note that Na may incorporated into the titanite structure (Table 11), whereas K is too large for the Ca-position in titanite (Shannon, 1976) and cannot be incorporated in any significant amounts.

The D^{Sm} from experiment SH2Na, where both Na_2O and Al_2O_3 were available, plotted exactly on the trend NBO/T versus D^{Sm} and ASI versus D^{Sm} (c.f., pentagons

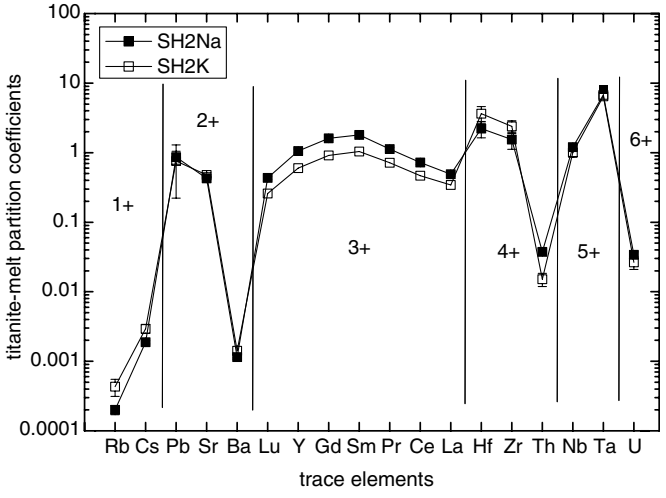

Fig. 7. Titanite/melt partition coefficients in two separate experiments with the same degree of polymerisation of melts, one (SH2Na) containing both Na and Al, the other (SH2K) containing K and Al. As K cannot be a coupled substitution partner for REE, we find generally lower partition coefficient for all elements influenced by coupled substitution. D^{Sr} and D^{Ba} for example, are not incorporated into titanite via coupled substitution and, hence, partition coefficients are not affected by either Na or K in the system. Error bars (1 sigma) only shown when larger than symbols.

in Fig. 5). In the experiment, where no Na_2O is available, i.e. in the system which only contained K_2O (SH2K), we find significantly lower D^{Sm} ($D^{Sm} = 1.04$) compared with $D^{Sm} = 1.80$ in the system with Na_2O. As titanites contain no K_2O (Table 10), we can safely exclude K as a potential substitution partner for the incorporation of Sm in titanite. This results in lower D^{Sm}-values and, consequently, also results in an earlier failure of Henry's law in a composition without Na_2O.

Summarizing, our observations indicate that Na_2O and Al_2O_3 are important substitution partners for the incorporation of REE into titanite in the Henry's law region. The absence of these potential substitution partners in experiments results in lower partition coefficients for all trace elements which are incorporated via coupled substitution. Furthermore, Al and Na also seem to control the onset of Henry's law in our experiments. However, we cannot rule out a possible role of intrinsic Ca-vacancies on the partition coefficients.

3.4.3. The effect of substitution mechanism on partition coefficients in the non-Henry's law region

Fig. 6 shows that the Na- and Al-content of titanite increases linearly when Sm is present as a major element. At lower Sm concentrations, the Al and Na-concentration are not related to Sm concentration. The transition between these two trends marked the limit of Henry's law. In a system with high REE concentrations (e.g., 8000 ppm of each REE) we do observe a clear 1:1 correlation between REE and Al+Na, which indicates that the coupled substitution of REE with Al and Na (Fig. 6A) controls partition coefficients outside the Henry's law region (Fig. 6).

3.5. Comparison with previous work and implications for the application of partition coefficients to natural rocks

Green and Pearson (1986) presented experimentally derived partition coefficients between titanite and melt for La, Sm, Er and Lu in different bulk compositions. All titanites in their study contain several wt% REE (between 1.5 and 21 wt% REE_2O_3). Based on their results, Green and Pearson (1986) concluded that the substitution mechanism $(Ca^{2+(VII)} + Ti^{4+(VI)} \leftrightarrow REE^{3+(VII)} + Al^{3+(VI)})$ is responsible for the incorporation of the REE into the titanite structure. To compare our results with Green and Pearson's data we plotted their D^{Sm} in Fig. 8. It is apparent that Green and Pearson's partition coefficients plot clearly below our observed trend (c.f, the dotted line), which indicates that Green and Pearson's partition coefficients do not follow Henry's law. This does not, however, in any way devaluate Green and Pearson's (1986) data as many naturally occurring titanites contain high concentrations of REE.

In order to apply experimentally determined partition coefficients to natural titanites, one needs to carefully consider the trace element concentrations in the system. We show that the onset of Henry's law critically depends on bulk composition and melt composition.

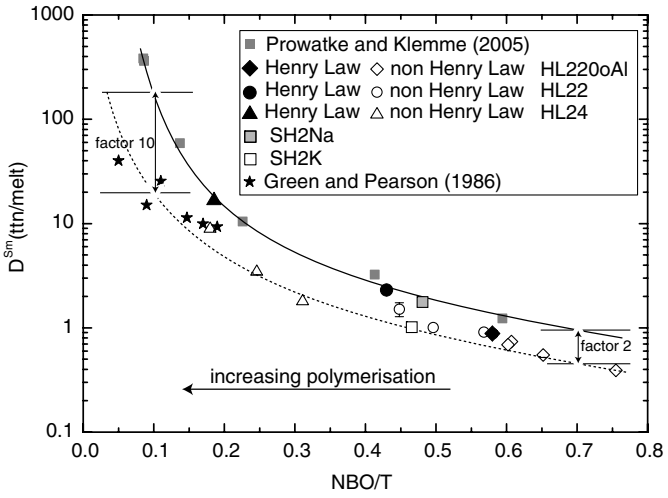

Fig. 8. Variation of D^{Sm} with increasing degree of polymerisation of melts. Two trends are shown. The upper trend (drawn as solid line) depicts experimental results in the Henry's law region. The lower trend (dotted line) shows experimental results outside Henrys law, where a substitution of Na and Al with Sm controls partitioning. The difference between Henry's law behaviour and non-Henry's law behaviour is much greater in systems with melts of high degree of polymerisation. Also plotted here are experiments by Green and Pearson (1986) which seem to be clearly outside Henry's law. Note that we used only Green and Pearson's experiments at 1000 and 1050 °C to ensure comparability. However, Green and Pearson's experiments were done at 1.0 GPa and a possible effect of pressure on partition coefficients, although unlikely, would result in increasing partition coefficients.

Natural magmatic titanites contain varying REE concentration ranging from traces (a few ppm) to several wt% (e.g., Paterson and Stephens, 1992; Seifert and Kramer, 2003; Vuorinen and Halenius, 2005; Seifert, 2005). For geochemical modelling of magmatic processes involving titanite, and indeed other accessory phases (Klemme et al., 2005; Prowatke et al., 2004; Prowatke and Klemme, 2006), it is of crucial importance to first evaluate whether the REE are present as traces or as major elements, only then appropriate D values may be chosen. Furthermore, it is also important to consider all elements that are incorporated in titanite by the same substitution mechanism as our experiments clearly show that Sm partition coefficients depend on the concentrations of the sum of all rare earth elements.

4. Conclusions

(1) Our experiments show that Henry's law of trace element partitioning depends on bulk composition, substitution mechanism, crystal composition, and melt composition.

(2) For a given bulk composition, titanite/melt partition coefficients are lower when Henry's law is not followed. This difference becomes larger with increasing polymerisation of the melt.

(3) The substitution mechanism and the availability of suitable substitution partners play an important role for trace element partitioning and also for the onset of Henry's law. Our results indicate that different substitution mechanisms operate for trace and for major elements.

(4) Our experiments indicate that the Henry's law region is significantly smaller when several elements are present that are incorporated by the same substitution mechanism or, in other words, we observe that Henry's law fails at much lower concentrations of one rare earth element when other REE are present.

Acknowledgments

We thank Drs. Horst Marschall and Dominik Hezel of the Erfolgsgruppe 2000, Rainer Altherr and Thomas Zack for discussions. The SIMS and electron microprobe analyses could not have been performed without generous help of Thomas Ludwig and Dr. Hans-Peter Meyer. We are indebted to Prof. D. Lattard for access to the experimental laboratories at Heidelberg University. We also thank Ilona Finn and Oliver Wienand for sample preparation. This work was supported by the Deutsche Forschungsgemeinschaft (KL1368/2-1) and the Leverhulme Trust. We also thank Dr. A. Corgne and an anonymous reviewer for reviews which helped to improve the manuscript substantially.

Associate editor: Brent T. Poe

References

Adam, J., Green, T.H., 1994. The effects of pressure and temperature on the partitioning of Ti, Sr and REE between amphibole, clinopyroxene and basanitic melts. *Chem. Geol.* **117**, 219–233.

Beattie, P., 1993. The occurrence of apparent non-Henry's law behaviour in experimental partitioning studies. *Geochim. Cosmochim. Acta* **57**, 47–55.

Bindeman, I.N., Davis, A.M., 2000. Trace element partitioning between plagioclase and melt: investigation of dopant influence on partition behavior. *Geochim. Cosmochim. Acta* **64**, 2863–2878.

Blundy, J.D., Wood, B.J., 1994. Prediction of crystal-melt partition coefficients from elastic moduli. *Nature* **372**, 452–454.

Corgne, A., Wood, B.J., 2005. Trace element partitioning and substitution mechanisms in calcium perovskites. *Contrib. Mineral. Petrol.* **149**, 85–97.

Corrigan, G., Gibb, F.G.F., 1979. Loss of Fe and Na from a basaltic melt during experiments using the wire-loop method. *Mineral. Mag.* **43**, 121–126.

Dinsdale, A.T., 1991. Thermal and physical properties of pure metals. *Calphad* **15**, 317.

Donaldson, C.H., Gibb, F.G.F., 1979. Changes in sample composition during experiments using the wire-loop technique. *Mineral. Mag.* **43**, 115–119.

Drake, M.J., Holloway, J.R., 1978. Henry law behavior of Sm in a natural plagioclase-melt system—importance of experimental procedure. *Geochim. Cosmochim. Acta* **42**, 679–683.

Green, T.H., Pearson, N.J., 1986. Rare-earth element partitioning between sphene and coexisting silicate liquid at high-pressure and temperature. *Chem. Geol.* **55**, 105–119.

Hanson, G.N., Langmuir, C.H., 1978. Modelling of major elements in mantle-melt systems using trace element approaches. *Geochim. Cosmochim. Acta* **42**, 725–741.

Harrison, W.J., 1981. Partitioning of REE between minerals and coexisting melts during partial melting of a garnet iherzolite. *Am. Mineral.* **66**, 242–259.

Harrison, W.J., Wood, B.J., 1980. An experimental investigation of the partitioning of REE between garnet and liquid with reference to the role of defect equilibria. *Contrib. Mineral. Petrol.* **72**, 145–155.

Hart, S.R., Davis, K.E., 1978. Nickel partitioning between olivine and silicate melt. *Earth Planet. Sci. Lett.* **40**, 203–219.

Klemme, S., Prowatke, S., Hametner, K., Günther, D., 2005. The partitioning of trace elements between rutile and silicate melts: Implications for subduction zones. *Geochem. Cosmochim. Acta* **69**, 2361–2371.

Mysen, B.O., 1978. Limits of solution of trace elements in minerals according to Henry's law: review of experimental data. *Geochim. Cosmochim. Acta* **42**, 871–885.

Nakada, S., 1991. Magmatic processes in titanite-bearing dacites, central Andes of Chile and Bolivia. *Am. Mineral.* **76**, 548–560.

Navrotsky, A., 1978. Thermodynamic of element partitioning: (1) systematics of transition metals in crystalline and molten silicates and (2) defect chemistry and "The Henry's law problem. *Geochim. Cosmochim. Acta* **42**, 887–902.

Paterson, B.A., Stephens, W.E., 1992. Kinetically induced compositional zoning in titanite: implications for accessory-phase/melt partitioning of trace elements. *Contrib. Mineral. Petrol.* **109**, 373–385.

Pearce, N.J.G., Perkins, W.T., Westgate, J.A., Gorton, M.P., Jackson, S.E., Neal, C.R., Chenery, S.P., 1997. A compilation of new and published major and trace element data for NIST SRM 610 and NIST SRM 612 glass reference material. *Geostand. Newslett.* **21**, 115–144.

Pouchou, J.L., Pichoir, F., 1984. A new model for quantitative analyses. I. Application to the analysis of homogeneous samples. *La Recherche Aérospatiale* **3**, 13–38.

Pouchou, J.L., Pichoir, F., 1985. 'PAP' procedure for improved quantitative microanalysis. *Microbeam Anal.* **54**, 104–106.

Prowatke, S., Klemme, S., 2005. Effect of melt composition on the partitioning of trace elements between titanite and melt. *Geochim. Cosmochim. Acta* **69**, 695–709.

Prowatke, S., Klemme, S., Ludwig, T., 2004. Experimental constraints on the partitioning of trace elements between apatite and silicate melts. *Lithos* **73**, S91.

Prowatke, S., Klemme, S., 2006. Trace element partitioning between apatite and silicate melts. *Geochim. Cosmochim. Acta* **70**, 4513–4527.

Ray, G.L., Shimizu, N., Hart, S.R., 1983. An ion microprobe study of the partitioning of trace elements between clinopyroxene and liquid in the system diopside–albite–anorthite. *Geochim. Cosmochim. Acta* **47**, 2131–2140.

Ribbe, P.H., 1980. Titanite. In: Ribbe, P.H. (Ed.), *Reviews in Mineralogy*, vol. 5. Mineralogical Society of America, USA, pp. 137–154.

Ryerson, F.J., Hess, P.C., 1978. Implications of liquid–liquid distribution coefficients to mineral–liquid partitioning. *Geochim. Cosmochim. Acta* **42**, 921–932.

Seifert, W., 2005. REE-, Zr-, and Th-rich titanite and associated accessory minerals from a kersantite in the Frankenwald, Germany. *Mineral. Petrol.* **84**, 129–146.

Seifert, W., Kramer, W., 2003. Accessory titanite: an important carrier of zirconium in lamprophyres. *Lithos* **71**, 81–98.

Shannon, R.D., 1976. Revised effective ionic radii and systematic studies of interatomic distances in halides and chalcogenides. *Acta Crystallographica.* **32**, 751–767.

Smith, A.L., 1970. Sphene, perovskite and coexisting Fe–Ti oxide minerals. *Am. Mineral.* **55**, 264–269.

Tiepolo, M., Oberti, R., Vannucci, R., 2002. Trace-element incorporation in titanite: constraints from experimentally determined solid/liquid partition coefficients. *Chem. Geol.* **191**, 105–119.

Urusov, V.S., Dudnikova, V.B., 1998. The trace-component trapping effect: experimental evidence, theoretical interpretation, and geochemical applications. *Geochim. Cosmochim. Acta* **62**, 1233–1240.

Veksler, I.V., Kogarko, L.N., Prigman, L.D., 1988. Phase-equilibria in the system sphene nepheline albite. *Geokhimiya* **8**, 1207–1220.

Vuorinen, J.H., Halenius, U., 2005. Nb-, Zr- and LREE-rich titanite from Alnö alkaline complex: crystal chemistry and its importance as petrogenetic indicator. *Lithos* **83**, 128–142.

Watson, E.B., 1976. 2-liquid partition-coefficients—experimental data and geochemical implications. *Contrib. Mineral. Petrol.* **56**, 119–134.

Watson, E.B., 1985. Henry law behavior in simple systems and in magmas—criteria for discerning concentration-dependent partition-coefficients in nature. *Geochim. Cosmochim. Acta* **49**, 917–923.

Wood, B.J., 1976. Samarium distribution between garnet and liquid at high pressure. *Carnegie Inst. Wash. Yearbook* **75**, 659–662.

Wood, B.J., Blundy, J.D., 1997. A predictive model for rare earth element partitioning between clinopyroxene and anhydrous silicate melt. *Contrib. Mineral. Petrol.* **129**, 166–181.